THE JOURNAL OF BIOLOGICAL CHEMISTRY VOL. 288, NO. 31, pp. 22248–22256, August 2, 2013

Brain-specific Angiogenesis Inhibitor-1 Signaling, Regulation, and Enrichment in the Postsynaptic Density*

Received for publication, May 30, 2013 Published, JBC Papers in Press, June 19, 2013, DOI 10.1074/jbc.M113.489757

Jason R. Stephenson[‡], Kevin J. Paavola[‡], Stacy A. Schaefer[‡], Balveen Kaur[§¶‖1], Erwin G. Van Meir[§¶‖], and Randy A. Hall[‡2]

From the [‡]Department of Pharmacology, Emory University School of Medicine, Atlanta, Georgia 30322, the [§]Laboratory of Molecular Neuro-oncology and [¶]Departments of Neurosurgery and Hematology & Medical Oncology, School of Medicine, and [‖]Winship Cancer Institute, Emory University, Atlanta, Georgia 30322

Background: BAI1 is an adhesion receptor; little is known about its signaling or localization.
Results: BAI1 activates Rho in a G protein-dependent manner, binds to synaptic scaffold proteins, and is highly enriched in the postsynaptic density.
Conclusion: BAI1 is a synaptic receptor that signals through G proteins.
Significance: BAI1 may play a previously unappreciated role as a regulator of synaptic function.

Brain-specific angiogenesis inhibitor-1 (BAI1) is an adhesion G protein-coupled receptor that has been studied primarily for its anti-angiogenic and anti-tumorigenic properties. We found that overexpression of BAI1 results in activation of the Rho pathway via a $G\alpha_{12/13}$-dependent mechanism, with truncation of the BAI1 N terminus resulting in a dramatic enhancement in receptor signaling. This constitutive activity of the truncated BAI1 mutant also resulted in enhanced downstream phosphorylation of ERK as well as increased receptor association with β-arrestin2 and increased ubiquitination of the receptor. To gain insights into the regulation of BAI1 signaling, we screened the C terminus of BAI1 against a proteomic array of PDZ domains to identify novel interacting partners. These screens revealed that the BAI1 C terminus interacts with a variety of PDZ domains from synaptic proteins, including MAGI-3. Removal of the BAI1 PDZ-binding motif resulted in attenuation of receptor signaling to Rho but had no effect on ERK activation. Conversely, co-expression with MAGI-3 was found to potentiate signaling to ERK by constitutively active BAI1 in a manner that was dependent on the PDZ-binding motif of the receptor. Biochemical fractionation studies revealed that BAI1 is highly enriched in post-synaptic density fractions, a finding consistent with our observations that BAI1 can interact with PDZ proteins known to be concentrated in the post-synaptic density. These findings demonstrate that BAI1 is a synaptic receptor that can activate both the Rho and ERK pathways, with the N-terminal and C-terminal regions of the receptor playing key roles in the regulation of BAI1 signaling activity.

The members of the adhesion family of G protein-coupled receptors (GPCRs)[3] are characterized by extremely large N-terminal regions containing modular adhesive domains and a GPCR proteolytic site (GPS) motif (1–3). Several adhesion GPCRs have been shown to undergo autoproteolysis at the GPS motif, which has been suggested from recent crystallographic data to be part of a much larger GPCR autoproteolysis-inducing domain (4). Following cleavage at the GPS motif, it has been shown for some members of this family that the cleaved N-terminal regions remain non-covalently associated with the seven-transmembrane (7TM) regions of the receptors for at least some period of time (2, 3).

BAI1 is a member of the adhesion GPCR family (5) and was initially identified in a screen for gene targets of the p53 tumor suppressor (6). It was subsequently determined that BAI1 is down-regulated in glioblastoma independently of p53 expression (7) through epigenetic regulation (8). BAI1 expression has been demonstrated in neurons, astrocytes, and macrophages (9–11), with lower levels of expression also being found in other tissues (12). Upon proteolysis at the GPS motif, BAI1 produces a 120-kDa N-terminal fragment, which has been named Vstat120 (vasculostatin 120) due to its ability to inhibit migration of endothelial cells (13). The growth of tumors derived from gliomas and renal cell carcinomas can be inhibited via restoration of BAI1 expression (14–17). The N terminus of BAI1 has also been shown to undergo further processing by a furin/matrix metalloproteinase-14 protease cascade to release a 40-kDa fragment, vasculostatin 40, which also inhibits angiogenesis (18). Furthermore, BAI1 has been shown to facilitate the engulfment of apoptotic cells via binding to externalized phosphatidylserine and activating Rac via recruitment of ELMO/Dock (10) and to promote myoblast fusion via the same pathway (19). Thus, BAI1 has been shown to signal in a G pro-

* This work was supported in part by National Institutes of Health Grants NS072394 (to R. A. H.) and CA086335 and CA163722 (to E. G. V. M.).

[1] Present address: Dardinger Laboratory for Neuro-oncology and Neurosciences, Department of Neurological Surgery, The Ohio State University Wexner Medical Center, Columbus, OH 43210.

[2] To whom correspondence should be addressed: Rollins Research Ctr., Rm. 5113, 1510 Clifton Rd., Emory University School of Medicine, Atlanta, GA 30322. Tel.: 404-727-3699; Fax: 404-727-0365; E-mail: rhall@pharm.emory.edu.

[3] The abbreviations used are: GPCR, G protein-coupled receptor; GPS, GPCR proteolytic site; RBD, Rho binding domain; BAI1, brain-specific angiogenesis inhibitor-1; NT, N terminus; CT, C terminus; PSD, postsynaptic density; 7TM, seven-transmembrane; RGS, regulator of G protein signaling; PDZ, postsynaptic density 95/discs-large/zona occludens-1; MAGI, membrane-associated guanylate kinase-like inverted.

tein-independent manner, but it remains unclear whether this receptor can also couple to G proteins to initiate a classical G protein-dependent signaling cascade.

In the present study, we sought to gain insight into the signaling and regulation of BAI1. Specifically, we examined whether BAI1 can couple to G proteins and whether receptor-signaling activity might be regulated by the large BAI1 N terminus. Additionally, we studied the potential regulation of BAI1 signaling by the C terminus of the receptor. The BAI1 C terminus has been reported to bind to two PDZ domain-containing scaffold proteins (20, 21), but nothing is known at present about the functional significance of these interactions. We sought to more comprehensively explore BAI1 associations with PDZ scaffolds and also assess the potential importance of these interactions in the regulation of receptor signaling. These studies led to a series of novel insights about the signaling, regulation, and subcellular localization of BAI1 and new ideas about the potential physiological importance of BAI1 *in vivo*.

EXPERIMENTAL PROCEDURES

Antibodies—Antibodies against HA (Roche Applied Science), FLAG (Sigma-Aldrich), β-arrestin2 (Cell Signaling), Myc (Sigma-Aldrich), PSD-95 (Thermo Scientific), synaptophysin (Abcam), BAI1 (Thermo Scientific), phospho-ERK (Santa Cruz Biotechnology), and total ERK (Cell Signaling Technology) were purchased from the manufacturers. A distinct anti-BAI1-CT antibody (antibody no. 17108) was custom-made by Pocono Rabbit Farm & Laboratory (Canadensis, PA) via injection of rabbits with a peptide (HSLTLKRDKAPKSS) derived from the human BAI1 C terminus (amino acids 1305–1318), followed by affinity purification.

Cell Culture and Transient Plasmid Transfections—HEK293T cells (ATCC) used for cell-based assays were cultured and maintained in complete medium (DMEM containing 10% FBS and 1% penicillin/streptomycin) at 37 °C at 5% CO_2. Transfections were performed by incubating cells plated on 100 × 20 mm cell culture dishes (Corning) with Lipofectamine 2000 (Invitrogen) and plasmid DNA for 3–5 h in serum-free DMEM. The transfection reaction was stopped by addition of complete medium. Experiments were performed 24 h post-transfection.

Plasmids—Expression vectors for BAI1 wild-type and Myc-BAI1-NT (Myc-Vstat120) were published previously (7, 13). The BAI1-ΔNT construct was cloned into pcDNA3.1 by creating primers for human BAI1 starting at amino acid 929 and ending at 1584. Primers used for PCR were 5′-GCTAGCATGTTCGCCATCTTAGCCCAGCTC-3′ and 5′-AAGCTTTCAGACCTCGGTCTGGAGGTCGAT-3′. The BAI1-ΔNTΔPDZ was cloned into pcDNA3.1 by creating primers from BAI1-ΔNT starting at amino acid 929 and ending at amino acid 1581. Primers used for PCR were 5′-GCTAGCATGTTCGCCATCTTAGCCCAGCTC-3′ and 5′-AAGCTTTCACTGGAGGTCGATGATGTCCTG-3′. The GST-BAI1-CT30 construct was made by cloning the sequence corresponding to the last 30 amino acids in the C terminus of BAI1 into the pGEX-4T1 vector using the following primers: 5′-GAATTCCCGCTGGAGCTTCGCAGCGTGGAGTGG-3′ and 5′-CTCGAGTCAGACCTCGGTCTGGAGGTCGATGAT-3′. The RGSp115 plasmid was a gift from Tohru Kozasa (University of Illinois at Chicago). The HA-ubiquitin construct was a gift from Keqiang Ye (Emory University). The GST-RBD (Addgene), FLAG-β-arrestin2 (Addgene), and HA-Rho (Missouri S&T cDNA Resource Center) expression vectors were all obtained from commercial sources.

Western Blot—Samples were run on 4–20% SDS-PAGE gels (Invitrogen) for 2 h at 130 V and then transferred to a nitrocellulose membrane (Bio-Rad) for 2 h at 30 V. The membrane was blocked in blot buffer containing 2% nonfat dry milk, 0.1% Tween 20, 50 mM NaCl, 10 mM Hepes, at pH 7.4 for 30 min at room temperature. The membrane was incubated with primary antibody in blot buffer for 1 h at room temperature, followed by three 5-min washes. The blots were then incubated with horseradish peroxidase-conjugated secondary antibody (GE Healthcare) for 30 min at room temperature followed by three 5-min washes with blot buffer. Blots were visualized via enzyme-linked chemiluminescence using the Supersignal® West Pico chemiluminescent substrate (Pierce). For phospho-ERK assessment, membranes were blocked in Odyssey blocking buffer and then incubated overnight with shaking at 4 °C with primary antibodies prepared in equal parts blocking buffer and PBS + 0.1% Tween 20. Nitrocellulose membranes were washed three times in PBS with 0.1% Tween 20 and incubated with Alexa Fluor anti-mouse 700 nm conjugated secondary antibody (1:20,000; Invitrogen) and anti-rabbit 800 nm conjugated secondary antibody (1:20,000; Li-Cor) for 30 min in equal parts blocking buffer and wash buffer. Blots were again washed three times and rinsed in PBS until being visualized on an Odyssey Imaging System (Li-Cor). Images were quantified using Image Station and ImageJ software.

Co-immunoprecipitation—Expression vectors for proteins of interest were transfected into HEK293T cells as described above. After 24 h, cells were resuspended in 500 μl of lysis buffer (1% Triton X-100, 150 mM NaCl, 25 mM Hepes, 10 mM $MgCl_2$, 1 mM EDTA, 1 protease inhibitor mixture tablet (Roche Diagnostics) and 2% glycerol). Cells were rotated in lysis buffer for 30 min at 4 °C, and then cell debris was cleared by centrifugation. Soluble lysates were incubated for 60 min with 30 μl of protein A/G beads (Thermo Scientific) with corresponding antibody (3 μl) to the protein being immunoprecipitated. Beads were washed 3 times with lysis buffer, resuspended in 40 μl of 2× sample buffer, and heated to 95 °C for 10 min.

Rhotekin Rho Activation Assay—HEK293T cells were co-transfected with expression plasmids for HA-Rho and either pcDNA3.1, BAI1 wild-type, BAI1-ΔNT, or BAI1-ΔNTΔPDZ with or without RGSp115. As described previously (22), 24 h post-transfection, cells were resuspended in 500 μl of lysis buffer. Cells were lysed by slowly rotating on a spinning wheel for 30 min at 4 °C, and then cell debris was cleared by centrifugation. Soluble cell lysates were incubated with 30 μl of GST-Rho binding domain (GST-RBD) of rhotekin coupled to glutathione-agarose beads (Sigma). Beads were washed three times with lysis buffer, resuspended in 40 μl of 2× sample buffer, and heated to 95 °C for 10 min. Active Rho was detected via the Western blot procedure described above. Images were quantified using ImageJ software.

PDZ Domain Proteomic Array—The PDZ domain proteomic array has been described previously (23, 24). Briefly, nylon membranes were spotted with bacterially produced recombinant His/S-tagged PDZ domain fusion proteins at a concentration of 1 μg per bin. Either control GST or a GST fusion protein corresponding to the last 30 amino acids of BAI1 were overlaid at a concentration of 100 nM in blot buffer overnight at 4 °C. The arrays were then washed three times with blot buffer and incubated with horseradish peroxidase-conjugated anti-GST antibody (Amersham Biosciences). Interactions of the GST fusion proteins and the PDZ domains were visualized by chemiluminescence using the ECL kit (Pierce).

Co-immunoprecipitation of PSD95·BAI1 Complex from Mouse Brain Homogenate—Brain tissue was extracted from adult mice and homogenized in ice-cold buffer containing 20 mM Hepes, pH 7.4, 50 mM NaCl, 1 mM EDTA, and a protease inhibitor mixture tablet (Roche Diagnostics). The resulting homogenate was then centrifuged at 2,000 × *g* for 10 min at 4 °C to remove nuclei and cell debris. Membrane proteins were extracted in Tris buffer (50 mM Tris, pH 7.4, 5 mM $MgCl_2$, 1 mM EGTA, 150 mM NaCl, 1 mM EDTA, one protease inhibitor mixture tablet, and 2% *n*-dodecyl-β-D-maltoside (Sigma) for 3 h at 4 °C, and debris was cleared by centrifugation. The resulting supernatant was rotated at 4 °C with protein A/G (Thermo Scientific) with or without anti-PSD95 antibody (Thermo Scientific) overnight. Protein A/G beads were washed three times with ice-cold buffer containing 20 mM Hepes, pH 7.4, 50 mM NaCl, 1 mM EDTA, and a protease inhibitor mixture tablet, resuspended in 40 μl of 2× sample buffer, and heated to 95 °C for 10 min. BAI1 and PSD95 were detected via the Western blot procedure described above.

GST Fusion Protein Pulldown Assay—GST fusion proteins were purified from bacteria using glutathione-Sepharose 4B beads (Sigma) and resuspended in resuspension buffer (50 mM NaCl, 10 mM Hepes, and 1 mM EDTA and 1 protease inhibitor mixture tablet (Roche Diagnostics)). Equal amounts of fusion proteins conjugated on beads were incubated with 500 μl of soluble lysates from HEK293T cells transfected with BAI1-ΔNT or BAI1-ΔNTΔPDZ for 60 min at 4 °C with rotation. The beads were extensively washed in lysis buffer, and proteins were eluted from beads in 40 μl of 2× sample buffer. Proteins were then resolved on SDS-PAGE and detected via Western blot as mentioned above.

ERK Phosphorylation Assay—HEK293T cells were transfected with pcDNA3.1, ΔNT, or ΔNTΔPDZ expression vectors with or without MAGI-3 expression vectors. 24 h post-transfection cells were serum-starved in Dulbecco's modified Eagle's medium (Invitrogen) for 2 h. Cells were then placed on ice and washed with ice-cold PBS. Following serum starvation, cells were harvested in 1.5× sample buffer and briefly sonicated. Protein lysates were resolved on SDS-PAGE, and proteins were visualized via Western blot and the Odyssey Imaging System as described above.

Cell Surface Biotinylation—HEK293T cells were transfected with BAI1 wild-type, ΔNT, or ΔNTΔPDZ expression vectors. 24 h post-transfection cells were placed on ice and washed with ice-cold PBS three times. Cells were then incubated with 10 mM Sulfo-NHS-SS-Biotin (Thermo Scientific) in PBS on ice for 1 h and then washed three times with PBS + 100 mM glycine. Cells were resuspended in 500 μl of lysis buffer and lysed by slowly rotating on a spinning wheel for 30 min at 4 °C. Cell debris was cleared by centrifugation, and soluble cell lysates were incubated with 30 μl of streptavidin agarose beads (Thermo Scientific) for 1 h. Beads were washed 3 times with lysis buffer, resuspended in 40 μl of 2× sample buffer, and heated to 95 °C for 10 min. Biotinylated constructs were detected via the Western blot procedure described above.

Preparation of Synaptosomes and Postsynaptic Density Fractions—As described previously (25), brain tissue was extracted from adult mice and homogenized in an ice-cold isotonic sucrose solution. The resulting homogenate was then centrifuged at 1,000 × *g* for 10 min at 4 °C to remove nuclei and cell debris. The supernatant was then placed on a Percoll (Sigma-Aldrich)/sucrose gradient and centrifuged at 31,000 × *g* for 5 min at 4 °C. The fraction located at the interface between the 15 and 23% Percoll gradient was extracted, diluted in ice-cold sucrose/EDTA (0.32 M sucrose, 1 mM EDTA, 5 mM Tris, pH 7.4), and centrifuged at 20,000 × *g* for 30 min at 4 °C. The pellet was resuspended in an isotonic buffer yielding the synaptosome fraction. The postsynaptic density fraction was then isolated via a 1% Triton X-100 extraction followed by high-speed centrifugation at 4 °C.

RESULTS

The BAI1 N-terminal and 7TM Regions Physically Associate—Similar to other adhesion GPCRs (2, 3, 22), BAI1 is known to be cleaved at the GPS motif in mouse brain lysates (4) and human malignant glioma cells (13, 17). However, it remains undetermined whether the two fragments of BAI1 can remain associated following cleavage of the receptor at the GPS. To determine whether the BAI1 7TM region can physically interact with the N-terminal region (also known as Vstat120) following cleavage, we created a truncated version of BAI1 (ΔNT) lacking the N-terminal region up to the predicted GPS cleavage site (Fig. 1*A*). When this construct was transfected into HEK293T cells, which are devoid of endogenous BAI1, the expressed protein migrated at its predicted molecular mass of 71 kDa (Fig. 1*B*). In contrast, transfection of HEK293T cells with full-length BAI1 resulted in a major band at ~200 kDa, which is consistent with past reports that BAI1 does not readily undergo autoproteolysis at the GPS motif in HEK293T cells (4, 26). To determine whether the BAI1 N-terminal and 7TM regions can interact, we performed co-immunoprecipitation studies utilizing the ΔNT construct and a Myc-tagged version of the BAI1-NT ("Vstat120") that we have described previously (13, 17). As shown in Fig. 1*C*, immunoprecipitation of Myc-BAI1-NT yielded co-immunoprecipitation of the co-expressed BAI1-ΔNT truncated mutant. These results indicate that the N-terminal and 7TM fragments of BAI1 can physically associate, even when co-transfected into cells as separate constructs.

BAI1 Signals to Rho via a $G\alpha_{12/13}$-dependent Pathway—To determine whether BAI1 can couple to G proteins, we transfected HEK293T cells with full-length BAI1 and assessed its ability to activate G protein-dependent signaling cascades. Because other adhesion GPCRs, including GPR56 (22, 27) and CD97 (28), have been found to robustly couple to $G\alpha_{12/13}$ to

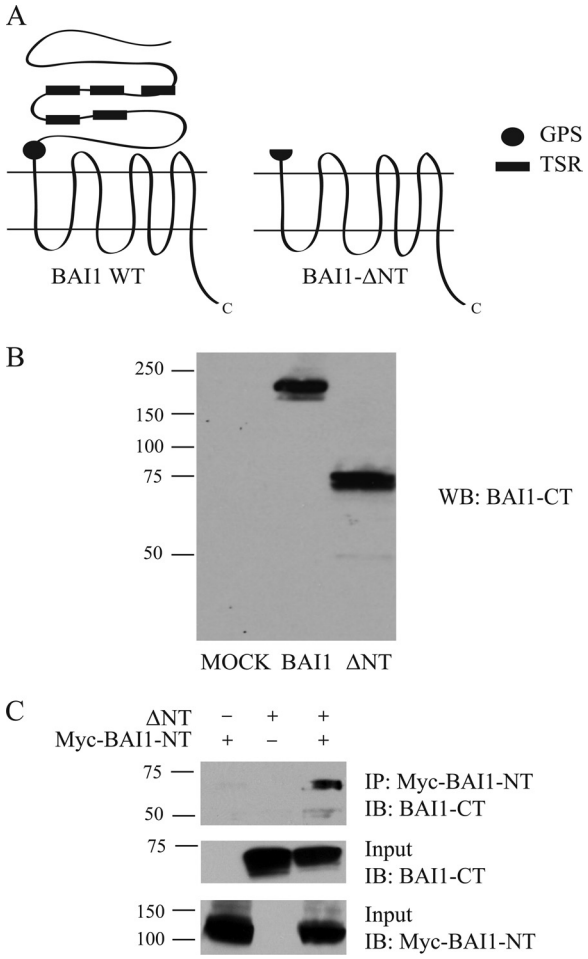

FIGURE 1. **Association between the N-terminal and 7TM regions of BAI1.** *A*, schematic drawing showing full-length BAI1 and the BAI1-ΔNT construct. *Rectangles* represent the thrombospondin-like repeats on the BAI1-NT, and the *circle* represents the GPS motif. *B*, lysates from HEK293T cells transiently transfected with either full-length BAI1 or BAI1-ΔNT were probed with anti-BAI1-CT antibody. The size of molecular mass markers is indicated in kDa. *C*, HEK293T cells were transiently transfected with a Myc-tagged expression vector for the N terminus of BAI1 (Myc-BAI1-NT) in the absence or presence of a second expression vector for BAI1 lacking the N terminus (BAI1-ΔNT). Immunoprecipitation (*IP*) was performed with an anti-Myc antibody bound to protein A/G beads. Co-immunoprecipitation of BAI1-ΔNT was detected via immunoblot (*IB*) with the anti-BAI1-CT antibody. Input lysates were examined as controls for protein amount and integrity. *WB*, Western blot; *NT*, N terminus.

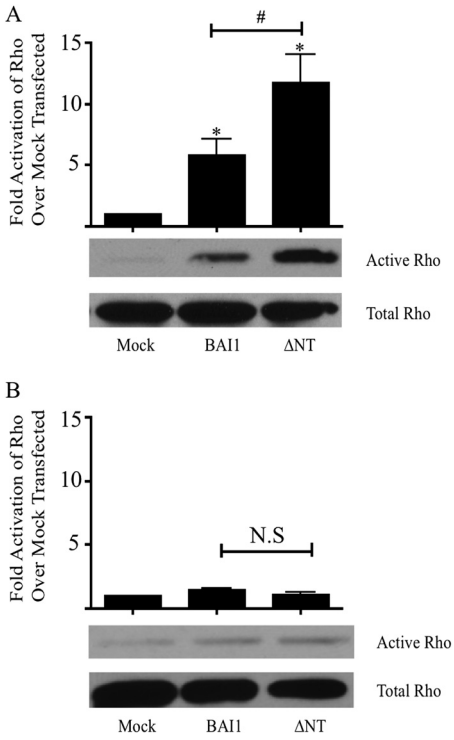

FIGURE 2. **BAI1 activates the Rho pathway via coupling to $G\alpha_{12/13}$.** *A*, quantification of active RhoA via pulldown with GST-RBD, a recombinant GST fusion protein corresponding to the Rho binding domain of rhotekin (*, comparison with mock-transfected; #, $p < 0.05$ ($n = 6$), one-way ANOVA). *Top*, Western blot analysis of active RhoA after pulldown with GST-RBD beads from HEK293T cells transiently transfected with empty vector (*Mock*), or expression vectors for full-length BAI1 or BAI1-ΔNT. *Bottom*, Western blot analysis of total RhoA levels in the input fraction of the same cells. *B*, quantification of active RhoA via pulldown with GST-RBD in the presence of RGSp115 (*N.S.*, not significant; $n = 3$, Student's *t* test). *Top*, Western blot analysis of active RhoA via pulldown with GST-RBD beads from HEK293T cells co-transfected with RGSp115 and either empty vector (*Mock*), full-length BAI1, or BAI1-ΔNT. *Bottom*, Western blot analysis of total RhoA levels in same cells. Refer to Fig. 1*B* for representative total expression levels of BAI1 and BAI1-ΔNT in HEK293T cells. *N.S.*, not significant; *NT*, N terminus.

activate Rho, we examined potential BAI1-mediated Rho signaling using a rhotekin pulldown assay (Fig. 2*A*). This assay uses the RBD of the Rho effector protein, rhotekin; the RBD motif binds specifically to the GTP-bound active form of Rho. When compared with cells transfected with empty vector ("mock"), a significant increase in Rho activation was observed upon transfection with full-length BAI1. Interestingly, transfection of cells with the BAI1-ΔNT mutant resulted in a significantly more robust activation of the Rho pathway than that observed with full-length BAI1. To determine whether the activation of Rho by BAI1 was mediated via receptor coupling to $G\alpha_{12/13}$, co-transfection with the regulator of G protein signaling (RGS) domain of p115RhoGEF (RGSp115) was used as a dominant-negative inhibitor for $G\alpha_{12/13}$-dependent signaling (29). RGSp115 specifically accelerates the GTPase activity of $G\alpha_{12/13}$, but not other G proteins, thereby selectively inhibiting $G\alpha_{12/13}$-mediated signaling. As shown in Fig. 2*B*, co-transfection with RGSp115 dramatically inhibited Rho activation by both full-length BAI1 and the BAI1-ΔNT mutant.

BAI1 Binds to a Variety of PDZ Domains from Synaptic Proteins—Because the C terminus of BAI1 contains a consensus sequence for possible interactions with PDZ domains (amino acids TEV), we screened a recombinant GST fusion protein corresponding to the last 30 amino acids of the BAI1-CT ("BAI1-CT30") against a proteomic array of 96 distinct PDZ domains to assess potential BAI1 interacting partners. As shown in Fig. 3*A*, interactions of the BAI1-CT30 were detected for PDZ1 + 2 of PSD-95 (bin B7) and PDZ4 + 5 of MAGI-1 (bin A4), consistent with previous reports (20, 21). Additionally, novel associations of the BAI1-CT were seen with PDZ domains from MAGI-2 (bin A8), MAGI-3 (bins B1 and B2), INADL (bin B12), SAP97 (bin C2), Chapsyn-110 (bin C6), MALS-1 (bin D9), Densin-180 (bin D11) PAPIN 1 (bin E11), and several syntrophins (bins E6–8, E10; Fig. 3*B*). In contrast to these positive hits detected with the BAI1-CT30, no significant labeling of the array was observed upon overlay of control GST. To assess whether these interactions might occur in native brain tissue, we performed co-immunoprecipitation experi-

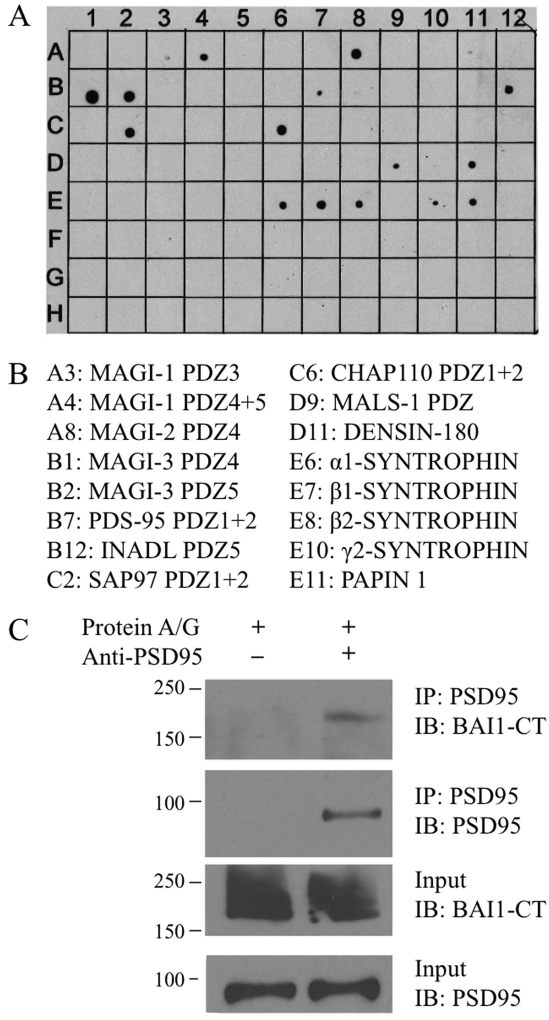

FIGURE 3. **BAI1 C terminus peptide binds selectively to PDZ domains from multiple synaptic proteins.** *A*, a recombinant GST fusion protein corresponding to the last 30 amino acids of BAI1 (GST-BAI1-CT30) was overlaid at 100 nM onto a proteomic array containing 96 distinct PDZ domains. The data shown are representative of three independent experiments. *B*, list of PDZ domains that interact with the GST-BAI1-CT30 fusion protein. The complete list of the PDZ proteins on this array has been described previously (23). *C*, co-immunoprecipitation (*IP*) of BAI1 and PSD-95 from mouse brain homogenates. Crude membrane fractions were collected by homogenization and centrifugation. Membrane proteins were solubilized in 2% dodecyl-β-D-maltoside, immunoprecipitated with protein A/G beads ± anti-PSD-95 antibodies, and probed via Western blot analyses with anti-BAI1-CT (Thermo Scientific) and anti-PSD-95 antibodies. *IB*, immunoblot.

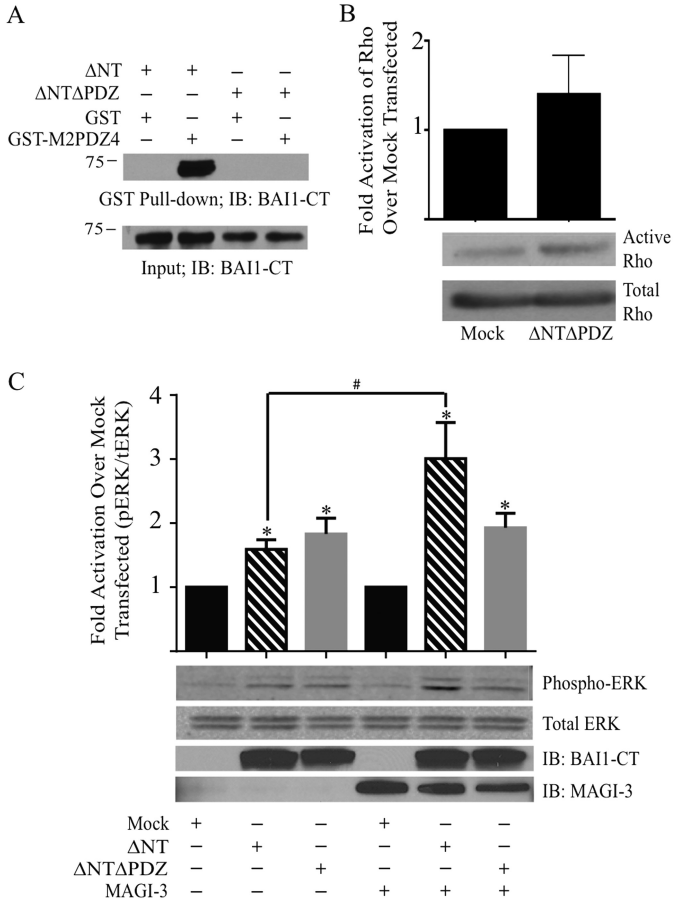

FIGURE 4. **Truncation of the PDZ-binding domain on the BAI1-CT disrupts binding to PDZ domains and differentially regulates signaling to Rho *versus* ERK.** *A*, a recombinant GST-MAGI-2 PDZ4 (GST-M2-PDZ4) fusion protein pulls down transfected BAI1-ΔNT but not the BAI1-ΔNTΔPDZ mutant from solubilized HEK293T cell lysates. *B*, quantification of active RhoA via pulldown with GST-RBD ($n = 4$). *Top*, immunoblot (*IB*) analysis of active RhoA following pulldown with GST-RBD beads from HEK293T cells transfected with empty vector (*Mock*) or expression vector for BAI1-ΔNTΔPDZ. *Bottom*, Western blot analysis of total RhoA levels in the same cells. *C*, quantification of phosphorylated ERK (pERK) to total ERK (tERK) from HEK293T cells transiently transfected with expression vectors for pcDNA3.1, BAI1-ΔNT, or BAI1-ΔNTΔPDZ with or without an expression vector for HIS-V5-MAGI-3 (*, comparison with mock-transfected; #, $p < 0.05$ ($n = 7$); one-way ANOVA). *Top panel*, immunoblot analysis of pERK. *Second panel*, immunoblot analysis of tERK. *Third panel*, immunoblot analysis of BAI1 from whole cell lysates. *Bottom panel*, immunoblot analysis of MAGI-3 from whole cell lysates. *NT*, N terminus.

ments examining whether complexes of BAI1 and PSD-95 could be detected in mouse brain homogenates. As shown in Fig. 3*C*, BAI1 was found to co-immunoprecipitate with PSD-95 in these studies, providing evidence for complex formation between these proteins in native brain tissue.

Removal of the BAI1 PDZ-binding Motif Attenuates BAI1-mediated Rho Signaling—To gain insights into the functional effects that PDZ interactions might have on the signaling and regulation of BAI1, the last three amino acids of the BAI1-CT (TEV) were truncated from the constitutively active BAI1-ΔNT construct ("BAI1-ΔNTΔPDZ"). To verify that removal of the BAI1 PDZ-binding motif indeed disrupts receptor interaction with PDZ domains, we utilized a pulldown assay with a recombinant GST fusion protein corresponding to PDZ4 from MAGI-2, which was one of the strongest interactions detected in the screen of the PDZ domain proteomic array (Fig. 3, bin A8). As shown in Fig. 4*A*, a strong association of MAGI-2 PDZ4 with the BAI1-ΔNT mutant was evident, whereas no detectable interaction was observed between MAGI-2 PDZ4 and the BAI1-ΔNTΔPDZ mutant, indicating that removal of the TEV sequence from the CT of BAI1 ablates the capacity of the receptor to interact with PDZ domains.

Next, the BAI1-ΔNTΔPDZ mutant receptor was assessed in terms of its ability to activate Rho. As shown in Fig. 4*B*, truncation of the BAI1 PDZ-binding motif greatly attenuated the ability of BAI1-ΔNT to activate Rho. No significant increase (1.3- ± 0.4-fold) in Rho activation compared with mock-transfected cells was observed following transfection with the BAI1-ΔNTΔPDZ expression vector.

MAGI-3 Potentiates BAI1-mediated ERK Activation only when the PDZ-binding Motif Is Intact—In addition to activating Rho, transfection of BAI1-ΔNT into HEK293 cells was found to result in a significant increase in ERK phosphorylation (Fig. 4*C*). Interestingly, BAI1-ΔNTΔPDZ caused a comparable increase in pERK, indicating that removal of the PDZ-binding motif exerts distinct effects on different BAI1-activated signaling pathways. Because MAGI-3 was found to robustly interact with BAI1 (Fig. 3, bins B1 and B2) and has been shown to regulate signaling to ERK by a variety of GPCRs, including the β_1AR (23), β_2AR (30), LPA(2) (31), and frizzled (32), we tested the effects of MAGI-3 co-expression on BAI1-mediated pERK signaling. Strikingly, MAGI-3 potentiated pERK levels when co-expressed with BAI1-ΔNT but had no effect at all on pERK stimulation mediated by BAI1-ΔNTΔPDZ.

Removal of the BAI1 N-terminal and PDZ-binding Motif Increases Receptor Association with β-Arrestin2 and Receptor Ubiquitination—Previous studies have shown that constitutively active receptors often exhibit robust interactions with β-arrestins, which dampen signaling by preventing receptor coupling to G proteins and promoting receptor internalization (33, 34). Thus, we assessed potential interactions of BAI1, BAI-ΔNT, and BAI1-ΔNTΔPDZ with arrestins. As shown in Fig. 5*A*, a significant interaction was seen between BAI1-ΔNT and β-arrestin2. In contrast, full-length BAI1 did not detectably bind to β-arrestin2. Interestingly, the BAI1-ΔNTΔPDZ mutant exhibited a level of β-arrestin2 interaction that was even more robust (3.5-fold higher) than that observed with the BAI1-ΔNT mutant, suggesting that PDZ protein binding to the C terminus may negatively regulate β-arrestin2 interactions.

Because constitutively active receptors can also be heavily ubiquitinated (35, 36), we co-transfected full-length BAI1, BAI1-ΔNT, or BAI1-ΔNTΔPDZ with HA-ubiquitin to determine levels of receptor ubiquitination. No observable ubiquitination of full-length BAI1 was seen. In contrast, significant and comparable levels of ubiquitination were observed for both BAI1-ΔNT and BAI1-ΔNTΔPDZ (Fig. 5*B*), indicating that removal of the PDZ-binding motif of BAI1 does not affect receptor ubiquitination. The observed differences in signaling activity, arrestin binding, and ubiquitination between full-length BAI1, BAI1-ΔNT, and the BAI1-ΔNTΔPDZ mutants could not be explained by deficient targeting of the mutant receptors to the plasma membrane, as cell surface biotinylation studies revealed comparable levels of plasma membrane localization between full-length BAI1, BAI1-ΔNT, and the BAI1-ΔNTΔPDZ mutants (Fig. 5*C*).

BAI1 Is Highly Enriched in the Postsynaptic Density—Because all of the PDZ domains found to interact with the BAI1-CT in the PDZ proteomic array screen were from synaptic proteins (Fig. 3), we assessed whether BAI1 might be enriched in synaptosomal (SYN) and/or postsynaptic density (PSD) fractions of mice brains. As shown in Fig. 6*A*, these studies revealed BAI1 to be somewhat enriched in synaptosomes but most strongly concentrated in PSD fractions, which is very similar to the pattern of enrichment observed for PSD-95, a known postsynaptic marker and one of the BAI1-interacting proteins detected in our proteomic screen. In contrast, immunoreactivity for synaptophysin, a presynaptic marker, was found to be enriched in synaptosomes but completely absent from the PSD fractions, thereby verifying the purity of the PSD fraction prepared for these experiments.

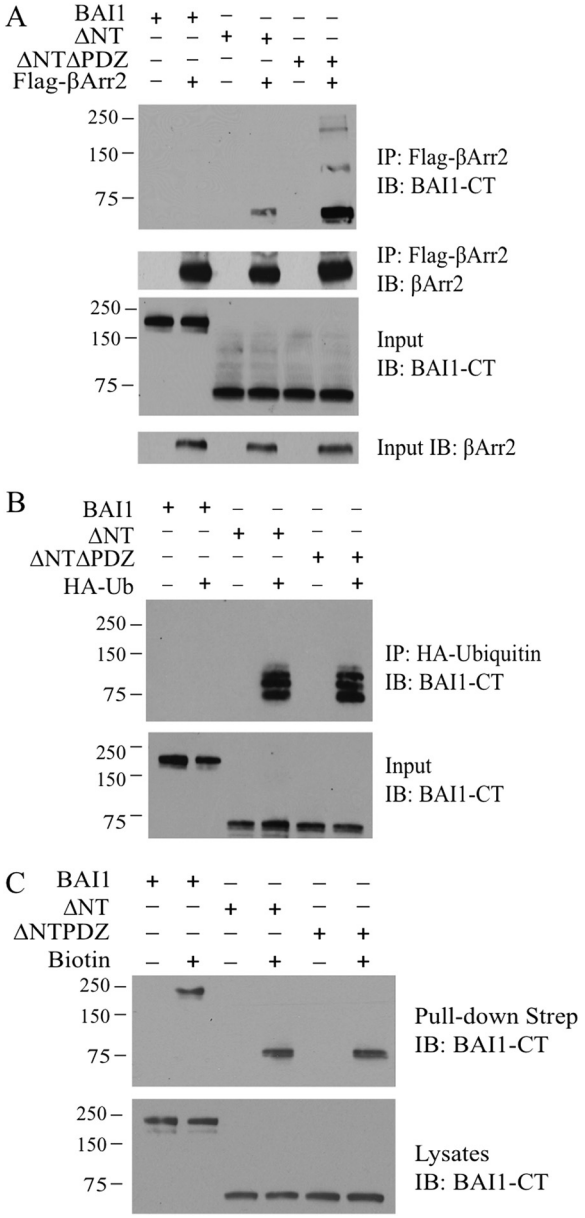

FIGURE 5. **Truncation of the PDZ-binding domain on the BAI1-CT enhances β-arrestin2 association but does not affect receptor ubiquitination.** *A*, HEK293T cells were transiently transfected with expression vectors for full-length BAI1, BAI1-ΔNT, or BAI1-ΔNTΔPDZ in the absence or presence of FLAG-β-arrestin2 (*βArr2*). Immunoprecipitation (*IP*) was performed with anti-FLAG antibody coupled to agarose beads. Co-immunoprecipitated BAI1 was detected by Western blot with anti-BAI1-CT antibody. *B*, expression vectors for full-length BAI1, BAI1-ΔNT, or BAI1-ΔNTΔPDZ were transiently co-transfected into HEK293T cells with an HA-ubiquitin (*HA-Ub*) expression vector. Immunoprecipitation was performed with anti-HA antibodies coupled to agarose beads. Co-immunoprecipitated BAI1 was visualized with anti-BAI1-CT antibody. *C*, HEK293T cells were transiently transfected with full-length BAI1, BAI1-ΔNT, or BAI1-ΔNTΔPDZ expression vectors and incubated with 10 mM Sulfo-NHS-ss-Biotin (*Biotin*). Biotinylated proteins, which represent proteins at the cell surface, and whole cell lysates (*WC lysates*) were visualized by Western blot using the anti-BAI1-CT antibody. *IB*, immunoblot; *NT*, N terminus; *CT*, C terminus; Strep, streptavidin.

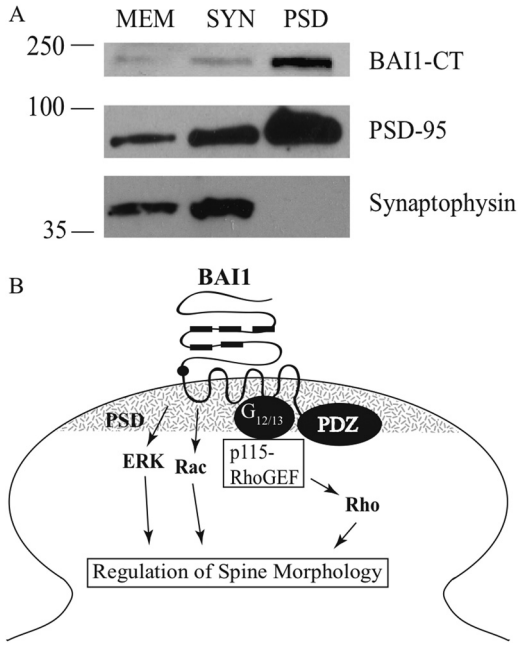

FIGURE 6. **BAI1 is enriched in the postsynaptic density.** *A*, synaptosome and postsynaptic density fractions were prepared from adult mice brains via a Percoll/sucrose gradient and 1% Triton X-100 extraction. Lysed crude membrane (*MEM*), synaptosome (*SYN*), and PSD fractions were probed via Western blot with antibodies for BAI1-CT (Thermo Scientific), PSD-95, and synaptophysin. Molecular masses of markers are indicated in kDa. *B*, schematic of the proposed role of BAI1 in the postsynaptic density. BAI1 is enriched in the PSD, signals through $G\alpha_{12/13}$ to activate the Rho pathway, and can also stimulate signaling to Rac and ERK. These signaling pathways can be regulated by BAI1 binding to a variety of PDZ domain-containing synaptic proteins. This model provides a mechanistic basis for BAI1-mediated regulation of synaptogenesis, dendritic spine integrity, and synaptic plasticity.

DISCUSSION

BAI1 has been studied for its anti-angiogenic and anti-tumorigenic properties in glial cells (5, 13, 17) as well as its ability to facilitate the engulfment of apoptotic cells (10) and induce myogenesis (19), but little is known about the signaling pathways by which BAI1 can mediate its various physiological actions. Here we report that BAI1 can activate the Rho pathway through coupling to $G\alpha_{12/13}$, thereby providing clear evidence that BAI1 does in fact couple to G proteins. These findings place BAI1 on the short list of adhesion GPCRs for which coupling to G proteins has been documented: GPR56 (22, 27) and CD97 (28) have been shown to activate Rho via $G\alpha_{12/13}$, latrophilin-1 has been shown to couple to $G\alpha_q$ and $G\alpha_o$ (37, 38), GPR133 (39) and GPR114 (40) have been shown to increase cAMP production through coupling to $G\alpha_s$, and GPR97 has been shown to couple to $G\alpha_o$ (40). Despite these recent advances in understanding the G protein coupling capabilities of adhesion GPCRs, there are still >20 members of the adhesion GPCR family about which nothing is known in terms of their G protein coupling preferences (2).

In addition to demonstrating G protein coupling by BAI1, we also provided evidence in the studies reported here that the NT and 7TM regions of BAI1 can physically interact with each other when cleaved apart at the GPS motif. In this regard, BAI1 is analogous to other members of the adhesion GPCR family for which it has been shown that the two fragments can remain associated following GPS cleavage (2, 3). Additionally, we found that removal of the BAI-NT results in enhanced receptor signaling activity, which suggests that the association of the BAI1-NT with the 7TM regions of the receptor results in suppression of BAI1 signaling activity. Similar inhibitory actions of the N termini of adhesion receptors have previously been reported for CD97 (28), GPR56 (22), and BAI2 (41). These congruent findings from work on four different receptors suggest a potentially general mechanism of activation for adhesion GPCRs, in which a receptor undergoes autoproteolysis, the N-terminal and 7TM regions remain associated for a period of time, and then ultimately, extracellular ligands bind to the NT and promote its disengagement from the 7TM region, which relieves the inhibitory constraint imposed by the N terminus and promotes receptor signaling activity. Other models of adhesion GPCR signaling have been proposed (42, 43), as, for example, it has been suggested that the N-terminal and 7TM regions of EMR2 are inactive when isolated but signal upon interaction within lipid rafts (44). Further work will be needed to clarify the activation mechanisms of adhesion GPCRs, but it is interesting to note that all current models focus on the importance of a dynamic interplay between the N-terminal and 7TM regions in regulating receptor signaling activity.

Through the use of a PDZ domain proteomic array, we found that the C terminus of BAI1 has the potential to bind to a variety of PDZ domains from synaptic proteins. Along with the previously-reported BAI1 interactions with PSD-95 (20) and MAGI-1 (21), novel interactions were seen in our PDZ domain screen with MAGI-2, MAGI-3, Densin-180, SAP97 (DLG1), MALS-1 (Veli-1), and several syntrophins. All of these proteins are localized to synapses (45–51). The ability of the BAI1-CT to selectively interact with PDZ domains from synaptic proteins suggests that BAI1 itself may be localized to synapses. Indeed, we found that BAI1 is highly enriched in postsynaptic density fractions prepared from adult mouse brain and that complexes between BAI1 and PSD-95 could be co-immunoprecipitated from brain tissue. Moreover, truncation of the BAI1 PDZ-binding motif resulted in an attenuation of receptor signaling to Rho but had no effect on receptor stimulation of pERK, revealing that PDZ scaffold interactions with BAI1 differentially regulate receptor coupling to the various signaling pathways that are downstream of the receptor. The importance of the PDZ-binding motif in regulating BAI1 signaling is further emphasized by our observations that MAGI-3 co-expression potentiated pERK activation by BAI1 only when the PDZ-binding motif was present. In terms of the mechanism(s) by which PDZ interactions might influence BAI1 signaling, we also observed that removal of the BAI1 PDZ-binding motif resulted in a sharp increase in receptor association with β-arrestin2. Because arrestins are known to impair G protein coupling to many different GPCRs (52) and also elicit their own signaling pathways, notably to ERK (53), it is possible that PDZ interactions with BAI1 could modulate receptor signaling by controlling the access of arrestins to the cytoplasmic regions of the receptor. Conversely, or perhaps concurrently, PDZ scaffolds might also recruit positive regulators of various signaling pathways into a complex with BAI1, thereby enhancing receptor signaling in a cell type-specific manner. The differential regulation of BAI1 by the various PDZ partners and β-arrestins in distinct cell

types and/or at different points in development will be an intriguing area for future exploration.

Our observation that BAI1 is highly enriched in the PSD is particularly interesting when considered in combination with our signaling data, which reveal that BAI1 can activate Rho via coupling to $G\alpha_{12/13}$. Rho GTPases are well established regulators of neuronal migration, synapse formation, PSD structure, and spine morphogenesis (54), as well as synaptic plasticity and memory formation (55). Along with Rho activation, we also observed BAI1-mediated increases in pERK, with this signaling being markedly enhanced in the presence of MAGI-3. Interestingly, ERK is known to play a key role in controlling the formation and stabilization of dendritic spines (56), thereby regulating synaptic plasticity, learning and memory (57, 58). While this manuscript was in revision, a paper was published revealing that BAI1 can regulate synaptogenesis via Rac activation through formation of a complex with the Rac-specific GEF Tiam1 (59). These data, along with our data presented here, represent an exciting step forward in revealing a previously unappreciated role for BAI1 as a master regulator of synapse formation and maintenance. We propose a model for BAI1 in which this receptor is enriched in the PSD and signals through multiple pathways including Rho, Rac and ERK to regulate synapse formation, spine morphogenesis, and synaptic plasticity (Fig. 6*B*). Our data furthermore reveal that the relative magnitudes of these BAI1-mediated signaling pathways can be influenced by BAI1 C-terminal interactions with various synaptic PDZ domain-containing proteins. Interestingly, the other two members of the BAI sub-family have also recently been implicated in the regulation of synaptic function and neural development: BAI2-deficient mice have been found to exhibit an enhanced rate of hippocampal neurogenesis (60), and BAI3 has been shown to interact with secreted complement-like C1q proteins to modulate synaptic density in cultured hippocampal neurons (61), and regulate dendrite morphogenesis (62). Thus, BAI1 and the other members of the BAI subfamily are emerging as important regulators of synaptic function and potentially attractive targets for therapeutics aimed at treating diseases associated with abnormalities of dendritic spines and synaptic plasticity, including schizophrenia, drug abuse, and neurodevelopmental disorders such as autism (63, 64).

Acknowledgments—We thank Luke Hartstein and William Watkins for technical support and Sarah Cork for helpful discussion.

REFERENCES

1. Bjarnadóttir, T. K., Fredriksson, R., and Schiöth, H. B. (2007) The adhesion GPCRs: a unique family of G protein-coupled receptors with important roles in both central and peripheral tissues. *Cell Mol. Life Sci.* **64,** 2104–2119
2. Paavola, K. J., and Hall, R. A. (2012) Adhesion G protein-coupled receptors: signaling, pharmacology, and mechanisms of activation. *Mol. Pharmacol.* **82,** 777–783
3. Yona, S., Lin, H. H., Siu, W. O., Gordon, S., and Stacey, M. (2008) Adhesion-GPCRs: emerging roles for novel receptors. *Trends Biochem. Sci.* **33,** 491–500
4. Araç, D., Boucard, A. A., Bolliger, M. F., Nguyen, J., Soltis, S. M., Südhof, T. C., and Brunger, A. T. (2012) A novel evolutionarily conserved domain of cell-adhesion GPCRs mediates autoproteolysis. *EMBO J.* **31,** 1364–1378
5. Cork, S. M., and Van Meir, E. G. (2011) Emerging roles for the BAI1 protein family in the regulation of phagocytosis, synaptogenesis, neurovasculature, and tumor development. *J. Mol. Med.* **89,** 743–752
6. Nishimori, H., Shiratsuchi, T., Urano, T., Kimura, Y., Kiyono, K., Tatsumi, K., Yoshida, S., Ono, M., Kuwano, M., Nakamura, Y., and Tokino, T. (1997) A novel brain-specific p53-target gene, BAI1, containing thrombospondin type 1 repeats inhibits experimental angiogenesis. *Oncogene* **15,** 2145–2150
7. Kaur, B., Brat, D. J., Calkins, C. C., and Van Meir, E. G. (2003) Brain angiogenesis inhibitor 1 is differentially expressed in normal brain and glioblastoma independently of p53 expression. *Am. J. Pathol.* **162,** 19–27
8. Zhu, D., Hunter, S. B., Vertino, P. M., and Van Meir, E. G. (2011) Overexpression of MBD2 in glioblastoma maintains epigenetic silencing and inhibits the antiangiogenic function of the tumor suppressor gene BAI1. *Cancer Res.* **71,** 5859–5870
9. Mori, K., Kanemura, Y., Fujikawa, H., Nakano, A., Ikemoto, H., Ozaki, I., Matsumoto, T., Tamura, K., Yokota, M., and Arita, N. (2002) Brain-specific angiogenesis inhibitor 1 (BAI1) is expressed in human cerebral neuronal cells. *Neurosci. Res.* **43,** 69–74
10. Park, D., Tosello-Trampont, A. C., Elliott, M. R., Lu, M., Haney, L. B., Ma, Z., Klibanov, A. L., Mandell, J. W., and Ravichandran, K. S. (2007) BAI1 is an engulfment receptor for apoptotic cells upstream of the ELMO/Dock180/Rac module. *Nature* **450,** 430–434
11. Sokolowski, J. D., Nobles, S. L., Heffron, D. S., Park, D., Ravichandran, K. S., and Mandell, J. W. (2011) Brain-specific angiogenesis inhibitor-1 expression in astrocytes and neurons: Implications for its dual function as an apoptotic engulfment receptor. *Brain Behav. Immun.* **25,** 915–921
12. Koh, J. T., Lee, Z. H., Ahn, K. Y., Kim, J. K., Bae, C. S., Kim, H. H., Kee, H. J., and Kim, K. K. (2001) Characterization of mouse brain-specific angiogenesis inhibitor 1 (BAI1) and phytanoyl-CoA alpha-hydroxylase-associated protein 1, a novel BAI1-binding protein. *Brain Res. Mol. Brain. Res.* **87,** 223–237
13. Kaur, B., Brat, D. J., Devi, N. S., and Van Meir, E. G. (2005) Vasculostatin, a proteolytic fragment of brain angiogenesis inhibitor 1, is an antiangiogenic and antitumorigenic factor. *Oncogene* **24,** 3632–3642
14. Xiao, X. R., Kang, X. X., and Zhao, J. Z. (2006) [Therapeutic effect of brain-specific angiogenesis inhibitor 1 on glioblastoma: an animal experiment]. *Zhonghua Yi Xue Za Zhi* **86,** 1342–1346
15. Kudo, S., Konda, R., Obara, W., Kudo, D., Tani, K., Nakamura, Y., and Fujioka, T. (2007) Inhibition of tumor growth through suppression of angiogenesis by brain-specific angiogenesis inhibitor 1 gene transfer in murine renal cell carcinoma. *Oncol. Rep.* **18,** 785–791
16. Yoon, K. C., Ahn, K. Y., Lee, J. H., Chun, B. J., Park, S. W., Seo, M. S., Park, Y. G., and Kim, K. K. (2005) Lipid-mediated delivery of brain-specific angiogenesis inhibitor 1 gene reduces corneal neovascularization in an *in vivo* rabbit model. *Gene Ther.* **12,** 617–624
17. Kaur, B., Cork, S. M., Sandberg, E. M., Devi, N. S., Zhang, Z., Klenotic, P. A., Febbraio, M., Shim, H., Mao, H., Tucker-Burden, C., Silverstein, R. L., Brat, D. J., Olson, J. J., and Van Meir, E. G. (2009) Vasculostatin inhibits intracranial glioma growth and negatively regulates *in vivo* angiogenesis through a CD36-dependent mechanism. *Cancer Res.* **69,** 1212–1220
18. Cork, S. M., Kaur, B., Devi, N. S., Cooper, L., Saltz, J. H., Sandberg, E. M., Kaluz, S., and Van Meir, E. G. (2012) A proprotein convertase/MMP-14 proteolytic cascade releases a novel 40 kDa vasculostatin from tumor suppressor BAI1. *Oncogene* **31,** 5144–5152
19. Hochreiter-Hufford, A. E., Lee, C. S., Kinchen, J. M., Sokolowski, J. D., Arandjelovic, S., Call, J. A., Klibanov, A. L., Yan, Z., Mandell, J. W., and Ravichandran, K. S. (2013) Phosphatidylserine receptor BAI1 and apoptotic cells as new promoters of myoblast fusion. *Nature* **497,** 263–267
20. Lim, I. A., Hall, D. D., and Hell, J. W. (2002) Selectivity and promiscuity of the first and second PDZ domains of PSD-95 and synapse-associated protein 102. *J. Biol. Chem.* **277,** 21697–21711
21. Shiratsuchi, T., Futamura, M., Oda, K., Nishimori, H., Nakamura, Y., and Tokino, T. (1998) Cloning and characterization of BAI-associated protein 1: a PDZ domain-containing protein that interacts with BAI1. *Biochem. Biophys. Res. Commun.* **247,** 597–604
22. Paavola, K. J., Stephenson, J. R., Ritter, S. L., Alter, S. P., and Hall, R. A. (2011) The N terminus of the adhesion G protein-coupled receptor GPR56 controls

receptor signaling activity. *J. Biol. Chem.* **286,** 28914–28921
23. He, J., Bellini, M., Inuzuka, H., Xu, J., Xiong, Y., Yang, X., Castleberry, A. M., and Hall, R. A. (2006) Proteomic analysis of β(1)-adrenergic receptor interactions with PDZ scaffold proteins. *J. Biol. Chem.* **281,** 2820–2827
24. Fam, S. R., Paquet, M., Castleberry, A. M., Oller, H., Lee, C. J., Traynelis, S. F., Smith, Y., Yun, C. C., and Hall, R. A. (2005) P2Y(1) receptor signaling is controlled by interaction with the PDZ scaffold NHERF-2. *Proc. Natl. Acad. Sci. U.S.A.* **102,** 8042–8047
25. Dunkley, P. R., Jarvie, P. E., and Robinson, P. J. (2008) A rapid Percoll gradient procedure for preparation of synaptosomes. *Nat. Protoc.* **3,** 1718–1728
26. Park, D., and Ravichandran, K. S. (2010) Emerging roles of brain-specific angiogenesis inhibitor 1. *Adv. Exp. Med. Biol.* **706,** 167–178
27. Iguchi, T., Sakata, K., Yoshizaki, K., Tago, K., Mizuno, N., and Itoh, H. (2008) Orphan G protein-coupled receptor GPR56 regulates neural progenitor cell migration via a $G\alpha_{12/13}$ and rho pathway. *J. Biol. Chem.* **283,** 14469–14478
28. Ward, Y., Lake, R., Yin, J. J., Heger, C. D., Raffeld, M., Goldsmith, P. K., Merino, M., and Kelly, K. (2011) LPA receptor heterodimerizes with CD97 to amplify LPA-initiated RHO-dependent signaling and invasion in prostate cancer cells. *Cancer Res.* **71,** 7301–7311
29. Kozasa, T., Jiang, X., Hart, M. J., Sternweis, P. M., Singer, W. D., Gilman, A. G., Bollag, G., and Sternweis, P. C. (1998) p115 RhoGEF, a GTPase activating protein for $G\alpha_{12}$ and $G\alpha_{13}$. *Science* **280,** 2109–2111
30. Yang, X., Zheng, J., Xiong, Y., Shen, H., Sun, L., Huang, Y., Sun, C., Li, Y., and He, J. (2010) β-2 adrenergic receptor mediated ERK activation is regulated by interaction with MAGI-3. *FEBS Lett.* **584,** 2207–2212
31. Zhang, H., Wang, D., Sun, H., Hall, R. A., and Yun, C. C. (2007) MAGI-3 regulates LPA-induced activation of Erk and RhoA. *Cell Signal* **19,** 261–268
32. Yao, R., Natsume, Y., and Noda, T. (2004) MAGI-3 is involved in the regulation of the JNK signaling pathway as a scaffold protein for frizzled and Ltap. *Oncogene* **23,** 6023–6030
33. Ferrari, S. L., and Bisello, A. (2001) Cellular distribution of constitutively active mutant parathyroid hormone (PTH)/PTH-related protein receptors and regulation of cyclic adenosine 3′,5′-monophosphate signaling by β-arrestin2. *Mol. Endocrinol.* **15,** 149–163
34. Mhaouty-Kodja, S., Barak, L. S., Scheer, A., Abuin, L., Diviani, D., Caron, M. G., and Cotecchia, S. (1999) Constitutively active α-1b adrenergic receptor mutants display different phosphorylation and internalization features. *Mol. Pharmacol.* **55,** 339–347
35. Shenoy, S. K., McDonald, P. H., Kohout, T. A., and Lefkowitz, R. J. (2001) Regulation of receptor fate by ubiquitination of activated β(2)-adrenergic receptor and β-arrestin. *Science* **294,** 1307–1313
36. Shenoy, S. K. (2007) Seven-transmembrane receptors and ubiquitination. *Circ. Res.* **100,** 1142–1154
37. Lelianova, V. G., Davletov, B. A., Sterling, A., Rahman, M. A., Grishin, E. V., Totty, N. F., and Ushkaryov, Y. A. (1997) α-Latrotoxin receptor, latrophilin, is a novel member of the secretin family of G protein-coupled receptors. *J. Biol. Chem.* **272,** 21504–21508
38. Rahman, M. A., Ashton, A. C., Meunier, F. A., Davletov, B. A., Dolly, J. O., and Ushkaryov, Y. A. (1999) Norepinephrine exocytosis stimulated by α-latrotoxin requires both external and stored Ca^{2+} and is mediated by latrophilin, G proteins and phospholipase C. *Philos. Trans. R. Soc. Lond. B Biol. Sci.* **354,** 379–386
39. Bohnekamp, J., and Schöneberg, T. (2011) Cell adhesion receptor GPR133 couples to G(s) protein. *J. Biol. Chem.* **286,** 41912–41916
40. Gupte, J., Swaminath, G., Danao, J., Tian, H., Li, Y., and Wu, X. (2012) Signaling property study of adhesion G-protein-coupled receptors. *FEBS Lett.* **586,** 1214–1219
41. Okajima, D., Kudo, G., and Yokota, H. (2010) Brain-specific angiogenesis inhibitor 2 (BAI2) may be activated by proteolytic processing. *J. Recept. Signal Transduct. Res.* **30,** 143–153
42. Araç, D., Aust, G., Calebiro, D., Engel, F. B., Formstone, C., Goffinet, A., Hamann, J., Kittel, R. J., Liebscher, I., Lin, H. H., Monk, K. R., Petrenko, A., Piao, X., Prömel, S., Schiöth, H. B., Schwartz, T. W., Stacey, M., Ushkaryov, Y. A., Wobus, M., Wolfrum, U., Xu, L., and Langenhan, T. (2012) Dissecting signaling and functions of adhesion G protein-coupled receptors. *Ann. N.Y. Acad. Sci.* **1276,** 1–25
43. Langenhan, T., Aust, G., and Hamann, J. (2013) Sticky signaling–adhesion class g protein-coupled receptors take the stage. *Sci. Signal.* **6,** re3
44. Huang, Y. S., Chiang, N. Y., Hu, C. H., Hsiao, C. C., Cheng, K. F., Tsai, W. P., Yona, S., Stacey, M., Gordon, S., Chang, G. W., and Lin, H. H. (2012) Activation of myeloid cell-specific adhesion class G protein-coupled receptor EMR2 via ligation-induced translocation and interaction of receptor subunits in lipid raft microdomains. *Mol. Cell. Biol.* **32,** 1408–1420
45. Apperson, M. L., Moon, I. S., and Kennedy, M. B. (1996) Characterization of densin-180, a new brain-specific synaptic protein of the *O*-sialoglycoprotein family. *J. Neurosci.* **16,** 6839–6852
46. Cho, K. O., Hunt, C. A., and Kennedy, M. B. (1992) The rat-brain postsynaptic density fraction contains a homolog of the *Drosophila* Disks-Large tumor suppressor protein. *Neuron* **9,** 929–942
47. Valtschanoff, J. G., Burette, A., Davare, M. A., Leonard, A. S., Hell, J. W., and Weinberg, R. J. (2000) SAP97 concentrates at the postsynaptic density in cerebral cortex. *Eur. J. Neurosci.* **12,** 3605–3614
48. Albrecht, D. E., and Froehner, S. C. (2002) Syntrophins and dystrobrevins: Defining the dystrophin scaffold at synapses. *Neurosignals* **11,** 123–129
49. Ito, H., Morishita, R., Sudo, K., Nishimura, Y. V., Inaguma, Y., Iwamoto, I., and Nagata, K. (2012) Biochemical and morphological characterization of MAGI-1 in neuronal tissue. *J. Neurosci. Res.* **90,** 1776–1781
50. Danielson, E., Zhang, N., Metallo, J., Kaleka, K., Shin, S. M., Gerges, N., and Lee, S. H. (2012) S-SCAM/MAGI-2 is an essential synaptic scaffolding molecule for the GluA2-containing maintenance pool of AMPA receptors. *J. Neurosci.* **32,** 6967–6980
51. Jo, K., Derin, R., Li, M., and Bredt, D. S. (1999) Characterization of MALS/Velis-1, -2, and -3: a family of mammalian LIN-7 homologs enriched at brain synapses in association with the postsynaptic density-95/NMDA receptor postsynaptic complex. *J. Neurosci.* **19,** 4189–4199
52. Reiter, E., and Lefkowitz, R. J. (2006) GRKs and β-arrestins: roles in receptor silencing, trafficking and signaling. *Trends Endocrinol. Metab.* **17,** 159–165
53. DeWire, S. M., Ahn, S., Lefkowitz, R. J., and Shenoy, S. K. (2007) β-arrestins and cell signaling. *Ann. Rev. Physiol.* **69,** 483–510
54. Tolias, K. F., Duman, J. G., and Um, K. (2011) Control of synapse development and plasticity by Rho GTPase regulatory proteins. *Prog. Neurobiol.* **94,** 133–148
55. Rex, C. S., Chen, L. Y., Sharma, A., Liu, J., Babayan, A. H., Gall, C. M., and Lynch, G. (2009) Different Rho GTPase-dependent signaling pathways initiate sequential steps in the consolidation of long-term potentiation. *J. Cell Biol.* **186,** 85–97
56. Goldin, M., and Segal, M. (2003) Protein kinase C and ERK involvement in dendritic spine plasticity in cultured rodent hippocampal neurons. *Eur. J. Neurosci.* **17,** 2529–2539
57. Giovannini, M. G. (2006) The role of the extracellular signal-regulated kinase pathway in memory encoding. *Rev. Neurosci.* **17,** 619–634
58. Sweatt, J. D. (2004) Mitogen-activated protein kinases in synaptic plasticity and memory. *Curr. Opin. Neurobiol.* **14,** 311–317
59. Duman, J. G., Tzeng, C. P., Tu, Y. K., Munjal, T., Schwechter, B., Ho, T. S., and Tolias, K. F. (2013) The adhesion-GPCR BAI1 regulates synaptogenesis by controlling the recruitment of the Par3/Tiam1 polarity complex to synaptic sites. *J. Neurosci.* **33,** 6964–6978
60. Okajima, D., Kudo, G., and Yokota, H. (2011) Antidepressant-like behavior in brain-specific angiogenesis inhibitor 2-deficient mice. *J. Physiol. Sci.* **61,** 47–54
61. Bolliger, M. F., Martinelli, D. C., and Südhof, T. C. (2011) The cell-adhesion G protein-coupled receptor BAI3 is a high-affinity receptor for C1q-like proteins. *Proc. Natl. Acad. Sci. U.S.A.* **108,** 2534–2539
62. Lanoue, V., Usardi, A., Sigoillot, S. M., Talleur, M., Iyer, K., Mariani, J., Isope, P., Vodjdani, G., Heintz, N., and Selimi, F. (2013) The adhesion-GPCR BAI3, a gene linked to psychiatric disorders, regulates dendrite morphogenesis in neurons. *Mol. Psych.*, DOI 10.1038/mp.2013.46 [Epub ahead of print]
63. Fiala, J. C., Spacek, J., and Harris, K. M. (2002) Dendritic spine pathology: Cause or consequence of neurological disorders? *Brain Res. Rev.* **39,** 29–54
64. Blanpied, T. A., and Ehlers, M. D. (2004) Microanatomy of dendritic spines: Emerging principles of synaptic pathology in psychiatric and neurological disease. *Biol. Psychiat.* **55,** 1121–1127